



Published in final edited form as:

Biochem J. 2012 April 1; 443(1): 259–266. doi:10.1042/BJ20111994.

Caveolae Optimize Tissue Factor-Factor VIIa Inhibitory Activity of Cell Surface Associated Tissue Factor Pathway Inhibitor

Susan A. Maroney^{*}, Paul E. Ellery^{*}, Jeremy P. Wood^{*}, Josephine P. Ferrel^{*}, Catherine E. Bonesho^{*}, and Alan E. Mast^{*,†}

^{*}Blood Research Institute, Blood Center of Wisconsin, Milwaukee, WI

[†]Department of Cell Biology, Neurobiology and Anatomy, Medical College of Wisconsin, Milwaukee, WI

Abstract

Tissue factor pathway inhibitor (TFPI) is an anticoagulant protein that prevents intravascular coagulation through inhibition of factor Xa (fXa) and the tissue factor (TF)-factor VIIa complex (TF-fVIIa). Localization of TFPI within caveolae enhances its anticoagulant activity. To further define how caveolae contribute to TFPI anticoagulant activity, CHO cells were co-transfected with TF and membrane associated TFPI targeted to either caveolae (TFPI-GPI) or to bulk plasma membrane (TFPI-TM). Stable clones had equal expression of surface TF and TFPI. TX-114 cellular lysis confirmed localization of TFPI-GPI to detergent insoluble membrane fractions, while TFPI-TM localized to the aqueous phase. TFPI-GPI and TFPI-TM were equally effective direct inhibitors of fXa in amidolytic assays. However, TFPI-GPI was a significantly better inhibitor of TF-FVIIa than TFPI-TM, as measured in both amidolytic and plasma clotting assays. Disrupting caveolae by removing membrane cholesterol from EA.hy926 cells, which make TFPI α , CHO cells transfected with TFPI β , and HUVECs, did not affect their fXa inhibition but significantly decreased their inhibition of TF-fVIIa. These studies confirm and quantify the enhanced anticoagulant activity of TFPI localized within caveolae, demonstrate that caveolae enhance the inhibitory activity of both TFPI isoforms, and define the effect of caveolae as specifically enhancing the anti-TF activity of TFPI.

Keywords

tissue factor; tissue factor pathway inhibitor; caveolae; lipid rafts; caveolin-1; membrane cholesterol

INTRODUCTION

Tissue factor pathway inhibitor (TFPI) is an anticoagulant protein that down regulates the initial stages of the blood coagulation cascade that is activated when tissue factor (TF) is exposed to flowing blood following either vascular injury or intravascular inflammation. TFPI is a multivalent Kunitz-type serine protease inhibitor mediating its anticoagulant activity by inhibiting factor Xa (fXa) via its second Kunitz domain and then producing feedback inhibition of the tissue factor-factor VIIa (TF-fVIIa) complex with the first Kunitz domain [1]. The physiological importance of TFPI may be best demonstrated by the embryonic lethal phenotype of mice lacking functional TFPI, with death caused by

unfettered TF procoagulant activity producing an apparent consumptive coagulopathy [2]. TFPI deficiency has not been identified in humans, suggesting that it results in embryonic death in humans as well as mice.

TFPI is an alternatively spliced protein with two forms identified in humans [3–5]. TFPI α is the full-length form. TFPI α associates with endothelium possibly through indirect binding to an, as yet, unidentified glycosylphosphatidyl inositol (GPI)-anchored binding protein [6–8]. In addition, heparin infusion produces a 2- to 4-fold increase in human plasma TFPI α [9,10]. This heparin releasable TFPI α probably associates non-specifically with endothelium glycosaminoglycans. Alternative splicing in the 3' end of the TFPI gene produces TFPI β , a truncated protein with a C-terminal domain distinct from TFPI α [4]. The C-terminal domain of TFPI β encodes a GPI-anchor binding sequence that allows for direct binding to the endothelial surface [11]. TFPI α and TFPI β both have the first and second Kunitz domains and inhibit TF-fVIIa and fXa activity in a variety of *in vitro* assays [3,11,12].

The association of TFPI with the cell surface via a GPI-anchor results in its localization within lipid raft microdomains on cellular surfaces [7,8,11] and suggests that lipid rafts may be important for their biological function. Lipid rafts are detergent insoluble areas of the cell membrane containing highly ordered glycosphingolipids and cholesterol that disrupt the relatively disordered, loosely packed phospholipids that compose the bulk phase cellular membrane. Caveolin-1 binds cholesterol [13] within lipid rafts and produces invaginated pits on the cell surface called caveolae [14]. Like lipid rafts, caveolae are disrupted by the chemical methyl- β -cyclodextrin (m- β -CD), which removes cholesterol from caveolin-1. When cholesterol is removed, caveolae flatten, lack intramembrane proteins, and move freely in a lateral direction within the membrane [15].

Caveolae are abundant on the surface of endothelial cells, the primary cellular source of TFPI, and caveolin-1 expression has been shown to enhance TFPI cell surface expression and anticoagulant activity [16]. Down regulation of TF-fVIIa procoagulant activity by TFPI on the cell surface coincides with translocation of the TF-fVIIa complex from the bulk-phase membrane into caveolae. Because caveolae inefficiently support TF-fVIIa activity, it has been hypothesized that the translocation acts to further down regulate TF-fVIIa procoagulant activity [8].

A previous study using HEK293 cells, which do not express caveolin-1, indicated that lipid rafts do not play a role in the down-regulation of TF activity by TFPI [17]. In order to better understand the role of caveolae in TFPI function, Chinese hamster ovary (CHO) cells, which produce abundant caveolin-1 [18], were transfected with TF, and then co-transfected with TFPI chimeras that attach TFPI to the cell surface either through a GPI-anchor (TFPI-GPI) or a transmembrane anchor (TFPI-TM). Cellular clones expressing equal amounts of TF and TFPI chimera were characterized for TFPI membrane localization and studied in fXa and TF-fVIIa initiated assay systems. The results demonstrate that localization of TFPI within caveolae does not impact inhibition of fXa activity, but substantially increases inhibition of TF-fVIIa.

EXPERIMENTAL

Cell culture

Chinese hamster ovary cells (CHO-K1) (ATCC, Manassas, VA) were cultured using F-12 medium (Mediatech, Inc., Manassas, VA). Human umbilical vein endothelial cells (HUVEC; Core Facility, BloodCenter of Wisconsin, Milwaukee, WI) and the EA.hy926 endothelial cell line (ATCC, Manassas, VA) were grown in MCDB-131 medium. All media

were supplemented with 10% fetal bovine serum (BioWest, Miami, FL), and endothelial cell media contained 1% penicillin/streptomycin (Mediatech, Inc., Manassas, VA) before use.

CHO cell transfection

Constructs encoding the TFPI chimeras TFPI-GPI or TFPI-TM, which contain amino acids 1–252 of human TFPI α followed by either a GPI-anchor target sequence from decay accelerating factor (TFPI-GPI) or a hydrophobic stretch of amino acids making up a transmembrane attachment from HLA-B44 (TFPI-TM), were as previously described [17]. The full length tissue factor (TF) construct was a gift from Dr Wolfram Ruf, M.D., (The Scripps Research Institute, La Jolla, CA). The region encoding TFPI β was amplified from human cDNA by PCR and ligated into the pDisplay plasmid (Invitrogen, Carlsbad, CA). CHO cells were transfected with the TF construct using Lipofectamine according to manufacturers' instructions (Invitrogen, Carlsbad, CA). Stable CHO-TF clones were produced using hygromycin and two rounds of cloning. They were screened by flow cytometry and a clone expressing high amounts of TF chosen to co-transfect with the TFPI-GPI, TFPI-TM, or TFPI β construct. Stable CHO-TF/TFPI-GPI, CHO-TF/TFPI-TM, and CHO-TF/TFPI β co-transfectants were selected using a combination of hygromycin and G-418. Cells were cloned and screened by flow cytometry to select clones expressing approximately equal amounts of TFPI-GPI, TFPI-TM, or TFPI β .

Standardization of cellular preparations

The concentrations of the different cellular clones used for most experiments were standardized through measurement of total protein (BCA Protein Assay Kit; Pierce, Rockford, IL). This was found to be a more accurate means for standardizing cell concentration than counting with a hemocytometer. Briefly, cells were seeded onto 100 mm tissue culture plates and grown to 90% confluence. They were washed with PBS and harvested with 10 mM EDTA in PBS containing protease inhibitors (50 μ M 3,4-DCI; 100 μ M E-64, Sigma, St Louis, MO) using a cell scraper. Cells were washed after centrifugation (182g, 15 minutes) then resuspended in 1 mL of PBS. A 100 μ L aliquot was pelleted by centrifugation and lysed in cell lysis buffer (30 mM CHAPS, 10 mM EDTA, in PBS) before assay. The remainder of the cell suspension remained on ice for approximately 2 hours before assay to allow the protease inhibitors to hydrolyze.

Phosphatidylinositol-specific Phospholipase C (PIPLC) cell treatment

Cells were harvested as described above then resuspended in PBS containing PIPLC (1 U/ml) (Invitrogen, Carlsbad, CA) and incubated for one hour at 37°C. Cells were centrifuged and collected for flow cytometric analysis.

Methyl- β -cyclodextrin (m- β -CD) cell treatment

Cells were grown to 90% confluence, harvested, re-suspended in the appropriate basal media without additives and incubated with 10 mM α -cyclodextrin (α -CD) or m- β -CD for 30 minutes at 37°C. They were centrifuged at 1200g for 10 minutes, washed with 1 mL of PBS, and resuspended in HEPES buffered saline albumin (HBSA; 50 mM HEPES, 100 mM NaCl, 10 mM CaCl₂, 0.1% BSA, pH 7.4) before assay.

Lipopolysaccharide (LPS) cell treatment

EA.hy926 and HUVE cells were treated with LPS to induce TF expression before determination of their potential to generate fXa in a TF-fVIIa dependent manner. Briefly, cells were grown to 80–90% confluence, washed with PBS, and incubated with 1 μ g/mL of LPS in the appropriate growth media for 6 hours at 37°C. Cells were harvested and prepared for assay as described.

Flow cytometry

Cells were harvested, standardized by cell count, fixed with 1.5% formaldehyde in PBS for 30 minutes, and incubated with primary antibody for 1 hour followed by secondary antibody for 30 minutes, with washes performed in between. The primary antibodies (10 µg/mL) used were mouse anti-human TFPI 2H8 antibody (a gift from Dr. George Broze, Washington University, St. Louis, MO), mouse anti-human TF (American Diagnostica, Stamford, CT), and mouse monoclonal isotype control antibody MOPC-21 (Sigma, St. Louis, MO). Alexa Fluor 488 (Fab')₂ goat anti-mouse IgG (1:500 dilution; Invitrogen, Carlsbad, CA) was used as the secondary antibody. Cells were analyzed using a BD LSRII Flow Cytometer and BD FACS Diva Software (BD Bioscience, San Jose, CA).

Triton X-114 phase separation and western blotting

Cells were harvested and lysed with 1 mL of Triton X-114 lysis buffer (10 mM Tris-HCl, 150 mM NaCl, 1 mM EDTA, 1% v/v Triton X-114, pH 7.4) for 1 hour at 4°C. The sample was centrifuged (20 000g, 10 min, 4°C) and the pellet saved for further analysis. The supernatant was collected, normalized to approximately 500 µg/mL total protein, and layered onto a sucrose cushion (6% sucrose, 0.06% Triton X-114 in PBS). It was incubated at 37°C for 3 minutes then centrifuged at 400g for 5 minutes at 30°C, separating the sample into an upper aqueous phase and lower detergent phase. The aqueous phase was collected for further analysis. The detergent phase was resuspended in 500 µL of PBS and phase separation repeated. The detergent rich phase was resuspended in 1 mL of cold PBS and saved for further analysis. The aqueous phases were pooled, 50 µL of 11.4% Triton X-114 added, and phase separation performed. The aqueous phase was saved for further analysis, while the detergent pellet was discarded. TFPI was isolated from all saved fractions by ligand-precipitation using fXa-coupled agarose beads, and subjected to SDS-PAGE and western blot analysis for TFPI as previously described [19].

¹²⁵I-fVIIa cell surface binding assay

Recombinant human fVIIa (Novo Nordisk A/S, Gentofte, Denmark) was labeled with ¹²⁵I to a specific activity of 6 × 10⁷ cpm/nmol fVIIa using IodoGen (Pierce, Rockford, IL) according to manufacturers' instructions. Cells were seeded after being normalized by total protein measurement and allowed to attach to the well of a 24-well plate overnight. They were washed with ice cold HBSA containing 11 mM glucose and 5 mM CaCl₂ and incubated with ¹²⁵I-fVIIa for 4 hours at 4°C. Cells were washed four times and bound ¹²⁵I-fVIIa removed with glycine (0.1M, pH 2.5) and quantified using a gamma counter (Packard Cobra Auto-Gamma, Perkin Elmer, MA, USA). Cells were incubated in the presence or absence of 100-fold molar excess of unlabeled fVIIa to determine binding specificity.

fXa inhibition assay

Cells were harvested, washed with PBS, and resuspended in HBSA containing 5 mM CaCl₂ (HBSA/Ca²⁺). Reaction conditions were prepared containing cells (varying concentrations, normalized to total protein) and factor Xa chromogenic substrate (0.5 mM; Spectrozyme Xa, American Diagnostica, Stamford, CT) in HBSA/Ca²⁺. Reactions were initiated by addition of fXa (0.1 nM), and substrate cleavage monitored at 405 nm for 45 minutes. Initial and final velocities were calculated from the progress curves between t=0 to 5 min and between t=40 to 45 min, respectively, and a factor Xa standard curve used to determine the amount of free factor Xa.

TF-fVIIa dependent fXa generation assay

Cells were harvested and mixed with fVIIa (0.02 nM for the TFPI inhibition assay in Figure 1E and 0.01 nM in all other figures) and fXa chromogenic substrate (500 µM). FX (20 nM)

(all final concentrations) was added and substrate cleavage monitored at 405nm for 1 hour. The maximal rate of substrate cleavage, calculated by SoftMAX Pro software, version 4.3.1 (Molecular Devices, Sunnyvale, CA), was compared to a standard curve generated using known amounts of fXa (2.5–51.6 nM) to calculate the maximal amount of fXa generated. Some experiments were performed following a 30 min incubation of the CHO cell clones with a monoclonal anti-TFPI antibody (100 µg/mL) directed against the second Kunitz domain (Novo Nordisk A/S, Denmark).

Plasma clotting assay

Plasma clotting assays were performed using human microparticle-poor plasma produced by centrifugation of platelet poor plasma at 200 000g for 1 hour. Cells were harvested and normalized to total protein. Cells, diluted in HBSA containing 38 mM CaCl₂, were added to a cuvette and the reaction started with 100 µL of plasma. The time to clot formation was determined using a STAT 4 coagulation analyzer (Diagnostics Stago, Parsippany, NJ).

Statistical analysis

To test for statistical significance, the students' *t*-test or one-way ANOVA were performed using GraphPad Prism for Windows, version 4.0. Bonferroni's Multiple Comparison test was performed to test for differences between groups when the one-way ANOVA was significant. A *p*-value less than 0.05 was considered statistically significant.

RESULTS

Characterization of transfected CHO cells

In order to study the role of caveolae in the inhibition of TF activity by TFPI, CHO cells, known to express caveolin-1 and contain caveolae [18], were first stably transfected with TF and then stably co-transfected with either the TFPI-GPI or TFPI-TM chimera. Flow cytometry analyses demonstrated that TF antigen expression was approximately equal on the selected clones (Figure 1A). Binding studies using ¹²⁵I-labelled fVIIa also were used to quantify TF on individual clones (Figure 1B). The three CHO cell lines transfected with TF bound nearly identical amounts of fVIIa, confirming that co-transfection of the cells with the TFPI chimera did not alter TF expression. Non-transfected, wild type CHO cells did not bind fVIIa confirming that the observed binding was TF dependent (Figure 1B). Similarly, the three cell lines generated similar amounts of fXa in a TF-dependent fXa generation assay when pre-treated with saturating amounts of anti-TFPI antibody (Figure 1C), confirming that they express essentially equal amounts of functional TF.

Flow cytometry for TFPI demonstrated similar amounts of TFPI antigen on the clones expressing TFPI (Figure 1D). Consistent with this finding, these clones exhibited similar total cell surface fXa inhibitory capacity (Figure 1E). A small fraction of the CHO cell clone expressing only TF also reacted with the TFPI antibody (Figure 1D). However, the absence of fXa inhibitory activity on these cells suggests that this is a non-specific reaction rather than endogenous CHO cell TFPI.

TFPI-GPI and TFPI-TM localize within different lipid environments

GPI-anchored proteins can be released from the cell surface by PIPLC, which cleaves the phosphoglycerol bond within the GPI-anchor [20]. The clones transfected with the TFPI chimeras were treated with PIPLC and removal of cell surface TFPI assessed by flow cytometry. PIPLC reduced TFPI antigen on the surface of cells transfected with TFPI-GPI by 93%, (Figure 2A) confirming that TFPI-GPI is GPI anchored [17, 21]. In contrast, PIPLC reduced TFPI antigen on the surface of cells transfected with TFPI-TM by only 13%, an

amount consistent with that removed during control reactions with PBS (Figure 2A and data not shown), confirming that it is transmembrane anchored [17].

Cellular lysis with TX-114 at 4°C was used to assess the lipid environment of TFPI-GPI and TFPI-TM. This separates cellular proteins into three phases – a detergent-insoluble, highly phospholipid-rich fraction which contains lipid rafts and associated proteins that precipitate at 4°C, and, after warming to 30°C, a detergent phase which contains phospholipid and membrane proteins, and an aqueous phase which contains soluble proteins and some membrane proteins [22]. Western blot analysis revealed differential localization of the TFPI chimeras (Figure 2B). The majority of TFPI-GPI was consistently present in the lipid raft pellet (Figure 2B, lane G), with the remainder in the detergent phase (Figure 2B, lane F). In contrast, TFPI-TM was found predominantly in the aqueous phase (Figure 2B, lane B). These results are again consistent with the localization of TFPI-GPI to lipid rafts [17, 21] and TFPI-TM to the bulk plasma membrane [17]. There was variability in western blot band intensity between the TFPI-GPI and TFPI-TM cells despite normalizing for total cellular protein prior to lysis with TX-114. This was not cell line specific as noted in repeated runs of this assay. Therefore, the differences in band intensity observed are likely due to variable protein loss during the fractionation procedure.

Inhibition of fXa by TFPI is not dependent on localization within caveolae

To assess if the localization of TFPI to caveolae contributes to its fXa inhibitory activity, CHO cells, expressing either TFPI-TM or TFPI-GPI, were incubated with fXa and cleavage of fXa chromogenic substrate monitored over time. Nearly identical progress curves were obtained with the two TFPI constructs, demonstrating that localization of TFPI within caveolae does not alter the rate of fXa inhibition (Figure 3). The initial (from t=0 to 5 min) and final (from t=40 to 45 min) reaction velocities were used to calculate the amount of uninhibited fXa at the initial stages of the reaction and at steady state, respectively (Table 1). Statistical analysis of these data demonstrated that there was no difference between TFPI-GPI and TFPI-TM ($p > 0.05$), confirming that the localization of TFPI to caveolae does not affect its direct fXa inhibitory activity.

Inhibition of TF-fVIIa mediated generation of fXa by TFPI is enhanced by caveolae

To determine if the TF-fVIIa inhibitory activity of cell surface TFPI is altered by localization to caveolae, the CHO cell clones were incubated with fVIIa and fX and the generation of fXa monitored over time (Figure 4A). Since these clones expressed greater amounts of TF than TFPI, fVIIa was used as the limiting reagent in these assays. The CHO cells expressing only TF generated a maximum fXa concentration of 45.3 ± 1.0 nM. This was reduced approximately 18% in cells expressing TFPI-TM to 37.3 ± 1.0 nM ($p < 0.001$ vs. CHO-TF cells) and by 37% in cells expressing TFPI-GPI to 28.4 ± 1.3 nM ($p < 0.001$ vs. CHO-TF cells). The maximum amount of fXa generated was reduced by 24% on the surface of cells expressing TFPI-GPI compared to those expressing TFPI-TM ($p < 0.001$) (Figure 4B).

Membrane cholesterol depletion reduces TFPI-GPI inhibitory activity to that of TFPI-TM

To further investigate the effect of TFPI localization to caveolae, fXa generation assays were repeated using CHO cell clones that had been treated with m- β -CD to remove cholesterol from the cell membrane. Treatment of the cells with α -CD, which does not remove membrane cholesterol, served as a comparative control. Previous studies have demonstrated that m- β -CD can increase [23] or decrease [24, 25] functional TF at the cell surface, depending on the cell type. Therefore, cyclodextrin treatment was first performed on CHO-TF cells to determine its effect on TF activity in this cell line. The maximum concentration of fXa generated was minimally decreased by α -CD compared to both m- β -

CD and a PBS control (38.1 ± 0.5 vs 40.5 ± 0.5 and 41.0 ± 0.8 nM, respectively, $p < 0.05$; and Figure 5A). The minor effect observed with α -CD may be due to perturbation of the bulk plasma membrane [26]. However, given that there was no difference in fXa generation between m- β -CD and PBS treated cells, it can be concluded that m- β -CD does not increase TF activity on the CHO cell surface.

M- β -CD treatment did not alter the amount of fXa generated for cells expressing TFPI-TM (Figure 5B, m- β -CD: 30.2 ± 2.2 versus α -CD: 30.6 ± 2.6 nM, $p > 0.05$), a finding that is again consistent with the localization of TFPI-TM within the bulk membrane. In contrast, m- β -CD treatment of CHO-TF cells expressing TFPI-GPI significantly increased the amount of fXa (Figure 5B, m- β -CD: 27.4 ± 0.7 nM vs. α -CD: 17.1 ± 1.3 nM, $p < 0.001$) almost to that observed for cells expressing TFPI-TM. It is noted that m- β -CD treatment may selectively release GPI-anchored proteins from the cell membrane [27], as has been previously observed with TFPI-GPI expressed in HEK293 cells [17]. No such release was observed with CHO-TF cells expressing TFPI-GPI, as assessed by flow cytometry post α -CD and m- β -CD treatment (data not shown), and therefore the increased fXa generation demonstrated with TFPI-GPI cells post- m- β -CD treatment is not due to loss of the inhibitor from the cell surface.

Inhibition of TF-fVIIa initiated plasma clotting by TFPI is enhanced by caveolae

TF-initiated plasma clotting assays were used to further assess the role of caveolae in TFPI anticoagulant activity. Cells expressing TFPI-TM increased the time to clot formation by 29% compared to cells expressing only TF (205.6 ± 18.6 seconds versus 158.8 ± 29.1 seconds, $p < 0.05$). Cells expressing TFPI-GPI increased the time to clot formation by 113% over CHO-TF cells (338.8 ± 32.2 seconds, $p < 0.001$), and by 65% over cells expressing TFPI-TM ($p < 0.001$) (Figure 6).

Caveolae enhance inhibition of TF-fVIIa, but not fXa, by the natural TFPI isoforms

The TFPI-GPI and TFPI-TM chimeras are altered forms of TFPI α . Endogenous TFPI is an alternatively spliced protein with two major isoforms produced in humans, TFPI α and TFPI β [5]. To investigate how caveolae alter the inhibitory activity of these isoforms, m- β -CD was used to deplete the membrane cholesterol of EA.hy926 cells, previously demonstrated to express TFPI α [19], and CHO-TF cells transfected with TFPI β . In addition, HUVECs were examined as a primary cell line that expresses TFPI, although the TFPI isoform expression has not been characterized. Again, treatment of the cells with α -CD served as a comparative control. Consistent with the CHO cell experiments, m- β -CD treatment of these cells did not affect their direct fXa inhibitory activity (Table 2). In contrast, m- β -CD treatment of these cells decreased their TF-fVIIa inhibitory activity in fXa generation assays (Figure 7). The greatest effect was observed with EA.hy926 cells, where m- β -CD resulted in a 67% increase in the amount of fXa generated (m- β -CD – 44.1 ± 5.5 vs. α -CD – 26.5 ± 4.2 nM, $p < 0.001$). The maximum amount of fXa generated was also significantly increased by m- β -CD treatment of HUVECs (41% increase, m- β -CD – 39.6 ± 2.9 vs. α -CD – 27.9 ± 1.5 nM, $p < 0.01$) and CHO-H β cells (18% increase, m- β -CD – 32.1 ± 1.6 vs. α -CD – 27.1 ± 1.3 nM, $p < 0.001$).

DISCUSSION

TFPI is a GPI-anchored protein that localizes within caveolae on the endothelial surface [7, 8, 11]. The presence of caveolae on the cell surface enhances TFPI anticoagulant activity and redistributes TF-fVIIa to detergent insoluble microdomains that contain lipids, which only weakly support procoagulant proteolytic reactions [8]. Here, we have produced CHO cell lines that express TF and either TFPI-GPI or TFPI-TM to further define and quantify the

enhancing effect of caveolae on TFPI anticoagulant activity. Studies with these cells demonstrate that localization of TFPI to caveolae enhances the inhibition of TF-fVIIa dependent fXa generation by approximately 30%, but has no effect on fXa inhibitory activity. This effect was also present, and perhaps more substantial, in plasma clotting assays, where TFPI localized to caveolae increased the time to clot formation by 65% compared to TFPI localized to the bulk membrane. Since the chimeras expressed in the CHO cells are altered forms of TFPI, cell lines expressing TFPI α and/or TFPI β were also studied to determine if caveolae enhance the anticoagulant activity of endogenous TFPI isoforms. In EA.hy926 cells, HUVECs, and CHO cells transfected with TFPI β , caveolae enhanced TFPI TF-fVIIa inhibitory activity but had no effect on fXa inhibitory activity, demonstrating that localization to caveolae enhances the anticoagulant activity of endogenously produced TFPI.

The second Kunitz domain of TFPI is a potent direct inhibitor of fXa [1]. The rate of inhibition is readily altered in solution phase assays by proteins or chemicals that interact with the third Kunitz domain or basic C-terminal region of TFPI α , including factor V, calcium, heparin [28, 29], and protein S [30, 31]. For example, calcium ions substantially decrease the K_i (initial) and K_i (final) for inhibition of fXa by blocking interactions between the C-terminus of TFPI α and the Gla domain of fXa [28, 29]. This decrease is abrogated when phospholipid and factor Va, or heparin are included in the assay system [28, 29]. In contrast to the variability in the rate of fXa inhibition observed in solution phase assays, the inhibition of fXa was not affected by the lipid environment of any cell surface associated form of TFPI examined here. Thus, the surrounding lipid composition of cell surface bound TFPI, and specifically its localization within caveolae, does not alter the accessibility of the second Kunitz domain to the active site of fXa.

While the second Kunitz domain of TFPI directly inhibits fXa, the first Kunitz domain is a fXa dependent inhibitor of TF-fVIIa [1]. Although these reactions are often described as being sequential with TFPI inhibiting fXa and then TFPI-fXa inhibiting TF-fVIIa, kinetic studies indicate that TFPI actually simultaneously inhibits fXa and TF-fVIIa in the ternary TF-fVIIa-fXa complex that forms immediately after fX is activated by TF-fVIIa [32]. Neither the C-terminal region of TFPI α [33] nor protein S [31], which localize soluble TFPI to phospholipid surfaces, enhance the inhibitory activity of soluble TFPI in reactions measuring the inhibition of fXa generation by TF-fVIIa. However, TFPI-GPI was a substantially better inhibitor of fXa generation than TFPI-TM and treatment with the cholesterol sequestering reagent, m- β -CD, decreased the inhibitory rate of TFPI-GPI to approximately that of TFPI-TM. Similarly, TFPI-GPI was a more potent anticoagulant than TFPI-TM in TF-initiated plasma clotting assays. Thus, localization within caveolae enhances inhibition of TF-fVIIa, but not fXa, by cell surface associated TFPI.

Studies by Awasthi and co-workers demonstrated that TF localizes within caveolae on the surface of MDA-MB-231 cells, however localization within caveolae was not necessary for its procoagulant activity [24]. We have reported that TFPI-GPI and TFPI-TM are equally effective inhibitors of TF-fVIIa mediated generation of fXa when expressed on the surface of HEK293 cells [17]. However, HEK293 cells do not express caveolin-1, and do not have caveolae [34, 35]. Therefore, it appears that lipid rafts alone do not enhance TFPI activity. Lupu and co-workers demonstrated that caveolin-1 transfection into HEK293 cells results in caveolae formation and decreased lateral mobility of TFPI on the cell surface perhaps enhancing its ability to interact with TF-fVIIa within caveolae [16]. These investigators further demonstrated that siRNA knockdown of caveolin-1 in HUVEC and EA.hy926 cells decreases cell surface TFPI expression and activity [16]. The present study investigating TFPI activity on CHO cells suggests that caveolin-1 alone is not sufficient for enhancing TFPI activity, as removal of membrane cholesterol decreased TFPI activity, while

maintaining expression of caveolin-1 at the cell surface [27, 36]. Therefore, it appears that the formation of caveolae is more important for enhancing TFPI anticoagulant activity than the lipid environment or caveolin-1 alone, perhaps caveolae localize TF and TFPI in cellular microdomains that allow for optimal recognition of TF-fVIIa by TFPI.

Studies using m- β -CD to disrupt caveolae in EA.hy926 cells, HUVECs and CHO cells expressing TFPI β were performed to investigate how caveolae alter the activity of TFPI α and TFPI β . As was observed with the TFPI chimeras expressed in CHO cells, caveolae enhanced the inhibition of TF-fVIIa, but not fXa, by endogenous TFPI forms produced by the three cell lines. In the cell models used here, caveolae enhanced the inhibitory activity of TFPI α to a greater degree than TFPI β because the m- β -CD associated increase in fXa generation in EA.hy926 cells, which produce TFPI α , was greater than that in the CHO cells transfected with TFPI β (67% versus 18%). However, it is likely that this difference is due to varying levels of TF and TFPI expression on the cell surface, resulting in different TF/TFPI ratios, as opposed to caveolae having a lesser effect on anticoagulant activity of TFPI β . Since TFPI α and TFPI β both associate with endothelium through a GPI-anchor and localize within caveolae, it is likely that the enhanced inhibition of TF-fVIIa by TFPI within caveolae is a physiologically relevant mechanism to prevent activation of blood coagulation within the vasculature.

Acknowledgments

SOURCES OF FUNDING

This work was supported by NHLBI grants HL068835 to AEM and HL091469 to SAM. JPW gratefully acknowledges training grant support from NHLBI grant HL007209. The content is solely the responsibility of the authors and does not necessarily represent the official views of the National Institutes of Health. Further support was provided through a research grant from Novo Nordisk to AEM.

ABBREVIATIONS

The abbreviations used are:

TF	Tissue Factor
TFPI	Tissue Factor Pathway Inhibitor
fVIIa	activated factor VII
TF-fVIIa	Tissue factor-factor VIIa complex
fXa	activated factor X
GPI	glycosylphatidylinositol
TFPI-GPI	GPI-anchored TFPI
TFPI-TM	transmembrane anchored TFPI
TX-114	Triton X-114
α-CD	α -cyclodextrin
m-β-CD	methyl- β -cyclodextrin
PI-PLC	phosphatidylinositol-specific phospholipase C
CHO	Chinese hamster ovary
HUVEC	human umbilical vein endothelial cell

REFERENCES

1. Girard TJ, Warren LA, Novotny WF, Likert KM, Brown SG, Miletich JP, Broze GJ Jr. Functional significance of the Kunitz-type inhibitory domains of lipoprotein-associated coagulation inhibitor. *Nature*. 1989; 338:518–520. [PubMed: 2927510]
2. Huang ZF, Broze G Jr. Consequences of tissue factor pathway inhibitor gene-disruption in mice. *Thromb Haemost*. 1997; 78:699–704. [PubMed: 9198242]
3. Maroney SA, Ferrel JP, Collins ML, Mast AE. Tissue factor pathway inhibitor-gamma is an active alternatively spliced form of tissue factor pathway inhibitor present in mice but not in humans. *J Thromb Haemost*. 2008; 6:1344–1351. [PubMed: 18503630]
4. Chang JY, Monroe DM, Oliver JA, Roberts HR. TFPIbeta, a second product from the mouse tissue factor pathway inhibitor (TFPI) gene. *Thromb Haemost*. 1999; 81:45–49. [PubMed: 9974373]
5. Maroney SA, Ellery PE, Mast AE. Alternatively spliced isoforms of tissue factor pathway inhibitor. *Thromb Res*. 2010; 125(Suppl 1):S52–S56. [PubMed: 20176395]
6. Mast AE, Acharya N, Malecha MJ, Hall CL, Dietzen DJ. Characterization of the association of tissue factor pathway inhibitor with human placenta. *Arterioscler Thromb Vasc Biol*. 2002; 22:2099–2104. [PubMed: 12482841]
7. Lupu C, Goodwin CA, Westmuckett AD, Emeis JJ, Scully MF, Kakkar VV, Lupu F. Tissue factor pathway inhibitor in endothelial cells colocalizes with glycolipid microdomains/caveolae. Regulatory mechanism(s) of the anticoagulant properties of the endothelium. *Arterioscler Thromb Vasc Biol*. 1997; 17:2964–2974. [PubMed: 9409283]
8. Sevinsky JR, Rao L, Ruf M. Ligand-induced protease receptor translocation into caveolae: A mechanism for regulating cell surface proteolysis of the tissue-factor dependent coagulation pathway. *J Cell Biol*. 1996; 133:293–304. [PubMed: 8609163]
9. Sandset PM, Abildgaard U, Larsen ML. Heparin induces release of extrinsic coagulation pathway inhibitor (EPI). *Thromb Res*. 1988; 50:803–813. [PubMed: 3413731]
10. Novotny WF, Brown SG, Miletich JP, Rader DJ, Broze GJ Jr. Plasma antigen levels of the lipoprotein-associated coagulation inhibitor in patient samples. *Blood*. 1991; 78:387–393. [PubMed: 2070076]
11. Zhang J, Piro O, Lu L, Broze GJ Jr. Glycosyl phosphatidylinositol anchorage of tissue factor pathway inhibitor. *Circulation*. 2003; 108:623–627. [PubMed: 12835228]
12. Piro O, Broze GJ Jr. Comparison of cell-surface TFPIalpha and beta. *J Thromb Haemost*. 2005; 3:2677–2683. [PubMed: 16246254]
13. Murata M, Peranen J, Schreiner R, Wieland F, Kurzchalia TV, Simons K. VIP21/caveolin is a cholesterol-binding protein. *Proceedings of the National Academy of Sciences of the United States of America*. 1995; 92:10339–10343. [PubMed: 7479780]
14. Rothberg KG, Heuser JE, Donzell WC, Ying YS, Glenney JR, Anderson RG. Caveolin, a protein component of caveolae membrane coats. *Cell*. 1992; 68:673–682. [PubMed: 1739974]
15. Westermann M, Steiniger F, Richter W. Belt-like localisation of caveolin in deep caveolae and its re-distribution after cholesterol depletion. *Histochem Cell Biol*. 2005; 123:613–620. [PubMed: 15889267]
16. Lupu C, Hu X, Lupu F. Caveolin-1 enhances tissue factor pathway inhibitor exposure and function on the cell surface. *J Biol Chem*. 2005; 280:22308–22317. [PubMed: 15817451]
17. Dietzen DJ, Jack GG, Page KL, Tetzloff TA, Hall CL, Mast AE. Localization of tissue factor pathway inhibitor to lipid rafts is not required for inhibition of factor VIIa/tissue factor activity. *Thromb Haemost*. 2003; 89:65–73. [PubMed: 12540955]
18. Mayor S, Maxfield FR. Insolubility and redistribution of GPI-anchored proteins at the cell surface after detergent treatment. *Mol Biol Cell*. 1995; 6:929–944. [PubMed: 7579703]
19. Maroney SA, Cunningham AC, Ferrel J, Hu R, Haberichter S, Mansbach CM, Brodsky RA, Dietzen DJ, Mast AE. A GPI-anchored co-receptor for tissue factor pathway inhibitor controls its intracellular trafficking and cell surface expression. *J Thromb Haemost*. 2006; 4:1114–1124. [PubMed: 16689766]

20. Sundler R, Alberts AW, Vagelos PR. Enzymatic properties of phosphatidylinositol inositolphosphohydrolase from *Bacillus cereus*. Substrate dilution in detergent-phospholipid micelles and bilayer vesicles. *J Biol Chem*. 1978; 253:4175–4179. [PubMed: 207692]
21. Ott I, Miyagi Y, Miyazaki K, Heeb MJ, Mueller BM, Rao LV, Ruf W. Reversible regulation of tissue factor-induced coagulation by glycosyl phosphatidylinositol-anchored tissue factor pathway inhibitor. *Arterioscler Thromb Vasc Biol*. 2000; 20:874–882. [PubMed: 10712416]
22. Pryde JG, Phillips JH. Fractionation of membrane proteins by temperature-induced phase separation in Triton X-114. Application to subcellular fractions of the adrenal medulla. *Biochem J*. 1986; 233:525–533. [PubMed: 2937402]
23. Dietzen DJ, Page KL, Tetzloff TA. Lipid rafts are necessary for tonic inhibition of cellular tissue factor procoagulant activity. *Blood*. 2004; 103:3038–3044. [PubMed: 15070681]
24. Awasthi V, Mandal SK, Papanna V, Rao LV, Pendurthi UR. Modulation of tissue factor-factor VIIa signaling by lipid rafts and caveolae. *Arteriosclerosis, Thrombosis, and Vascular Biology*. 2007; 27:1447–1455.
25. Mandal SK, Iakhiaev A, Pendurthi UR, Rao LVM. Acute cholesterol depletion impairs functional expression of tissue factor in fibroblasts: modulation of tissue factor activity by membrane cholesterol. *Blood*. 2005; 105:153–160. [PubMed: 15328160]
26. Ohtani Y, Irie T, Uekama K, Fukunaga K, Pitha J. Differential effects of alpha-, beta- and gamma-cyclodextrins on human erythrocytes. *Eur J Biochem*. 1989; 186:17–22. [PubMed: 2598927]
27. Ilangumaran S, Hoessli DC. Effects of cholesterol depletion by cyclodextrin on the sphingolipid microdomains of the plasma membrane. *Biochem J*. 1998; 335(Pt 2):433–440. [PubMed: 9761744]
28. Huang ZF, Wun TC, Broze GJ Jr. Kinetics of factor Xa inhibition by tissue factor pathway inhibitor. *J Biol Chem*. 1993; 268:26950–26955. [PubMed: 8262929]
29. Lockett JM, Mast AE. Contribution of regions distal to glycine-160 to the anticoagulant activity of tissue factor pathway inhibitor. *Biochemistry*. 2002; 41:4989–4997. [PubMed: 11939795]
30. Hackeng TM, Sere KM, Tans G, Rosing J. Protein S stimulates inhibition of the tissue factor pathway by tissue factor pathway inhibitor. *Proc Natl Acad Sci USA*. 2006; 103:3106–3111. [PubMed: 16488980]
31. Ndonwi M, Broze G Jr. Protein S enhances the tissue factor pathway inhibitor inhibition of factor Xa but not its inhibition of factor VIIa-tissue factor. *J Thromb Haemost*. 2008; 6:1044–1046. [PubMed: 18419747]
32. Baugh RJ, Broze GJ Jr, Krishnaswamy S. Regulation of extrinsic pathway factor Xa formation by tissue factor pathway inhibitor. *J Biol Chem*. 1998; 273:4378–4386. [PubMed: 9468488]
33. Petersen JG, Meyn G, Rasmussen JS, Petersen J, Bjorn SE, Jonassen I, Christiansen L, Nordfang O. Characterization of human tissue factor pathway inhibitor variants expressed in *Saccharomyces cerevisiae*. *J Biol Chem*. 1993; 268:13344–13351. [PubMed: 8514773]
34. Feng X, Gaeta ML, Madge LA, Yang JH, Bradley JR, Pober JS. Caveolin-1 associates with TRAF2 to form a complex that is recruited to tumor necrosis factor receptors. *J Biol Chem*. 2001; 276:8341–8349. [PubMed: 11112773]
35. Xu J, Qu D, Esmon NL, Esmon CT. Metalloproteolytic release of endothelial cell protein C receptor. *J Biol Chem*. 2000; 275:6038–6044. [PubMed: 10681599]
36. Hanada K, Nishijima M, Akamatsu Y, Pagano RE. Both sphingolipids and cholesterol participate in the detergent insolubility of alkaline phosphatase, a glycosylphosphatidylinositol-anchored protein, in mammalian membranes. *J Biol Chem*. 1995; 270:6254–6260. [PubMed: 7890763]

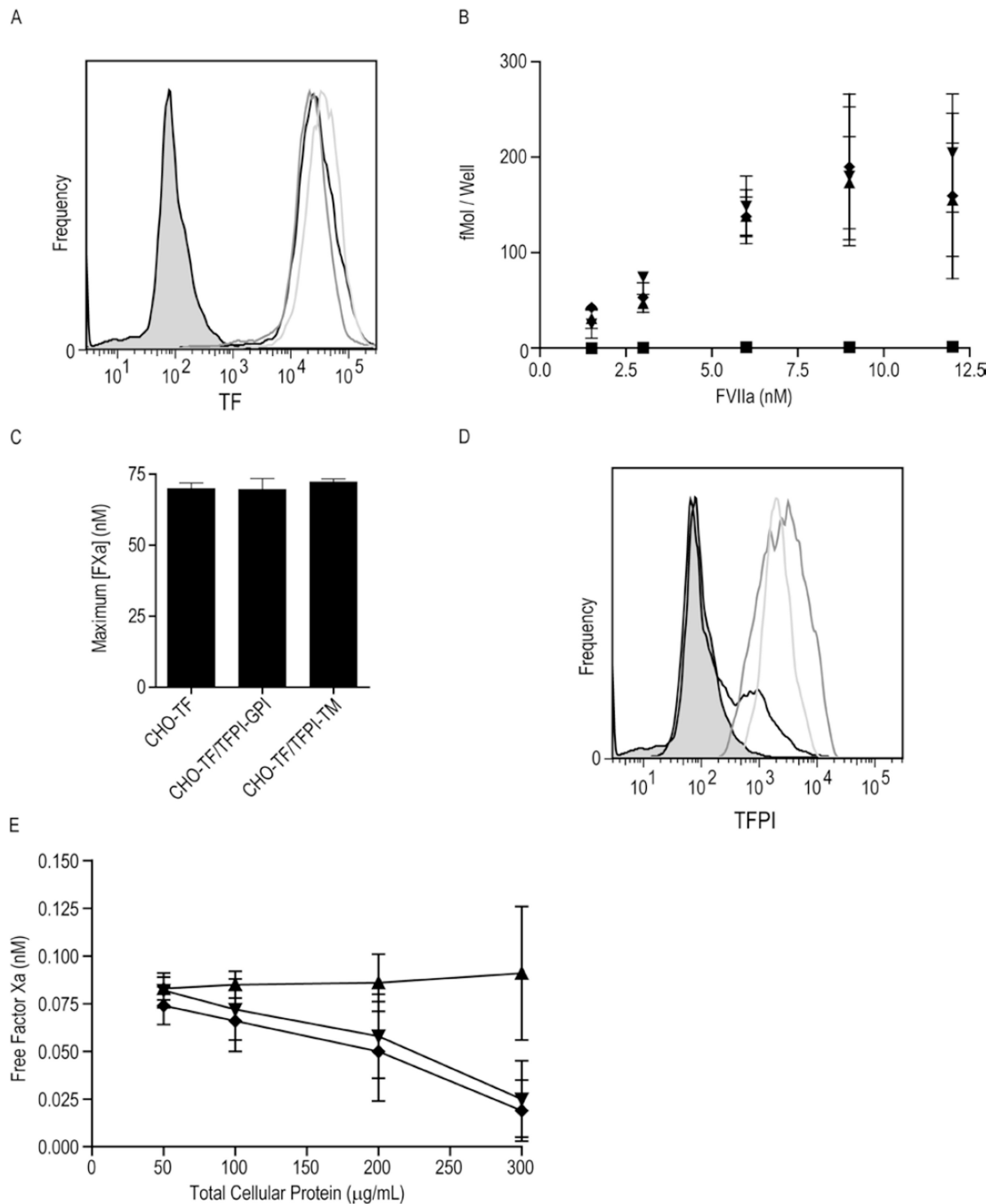


Figure 1. TF and TFPI expression on CHO-TF, CHO-TF/TFPI-GPI and CHO-TF/TFPI-TM cells

A) Flow cytometric analysis of cell surface TF expression on CHO-TF (black), CHO-TF/TFPI-GPI (dark grey) and CHO-TF/TFPI-TM (light grey) cells. The MOPC isotype control is shaded grey. B) ¹²⁵I-fVIIa binding to CHO-TF (▲), CHO-TF/TFPI-GPI (▼), CHO-TF/TFPI-TM (◆), and wild-type CHO cells (■); mean ± SD, n=4. C) Maximum concentration of fXa generated by CHO-TF, CHO-TF/TFPI-GPI, and CHO-TF/TFPI-TM cells (equivalent concentration of 300 μg/mL total cellular protein) pre-treated with 100 μg/mL monoclonal anti-TFPI antibody directed against the second Kunitz domain, assessed using the TF-fVIIa initiated fXa generation assay; mean ± SD, n=4. The assay was performed with cells in

suspension. D) Flow cytometric analysis of cell surface TFPI on CHO-TF (black), CHO-TF/TFPI-GPI (dark grey) and CHO-TF/TFPI-TM (light grey) cells. The MOPC isotype control is shaded gray. E) Factor Xa inhibitory activity of CHO-TF/TFPI-GPI (▼), CHO-TF/TFPI-TM (◆) and CHO-TF (▲) cells in suspension at the indicated cellular concentrations; mean \pm SD, n=6.

\$watermark-text

\$watermark-text

\$watermark-text

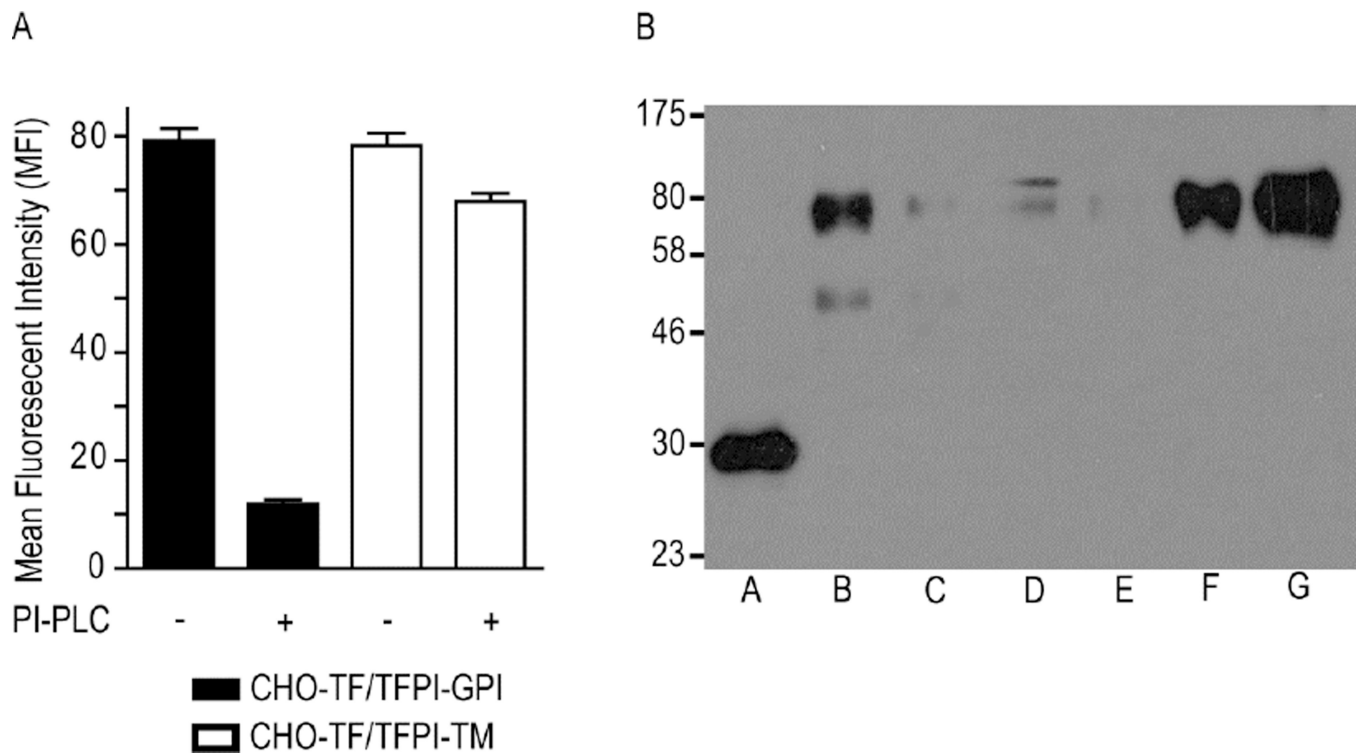


Figure 2. TFPI-GPI is localized to caveolae, while TFPI-TM is localized to the bulk plasma membrane

A) Flow cytometric analysis of TFPI expression on CHO-TF/TFPI-GPI and CHO-TF/TFPI-TM cells before and after PI-PLC treatment; mean \pm SD, n=4. B) Triton X-114 phase separation was performed on CHO-TF/TFPI-TM (Lanes B–D) and CHO-TF/TFPI-GPI cells (Lanes E–G), and the fractions analyzed for TFPI expression by Western blotting. Lane A: recombinant TFPI (32 kDa), expressed in *E. coli* and run as an antibody positive control; Lanes B and E: TX-114 aqueous phase; Lanes C and F: TX-114 detergent phase; Lanes D and G: TX-114 detergent insoluble pellet. The chimeras migrate to approximately 70 kDa, similar to that reported previously [17]. The lower band in lane B is a possible degradation product, while the upper band in lane D may be dimerization of the chimera [17] or a non-specific product.

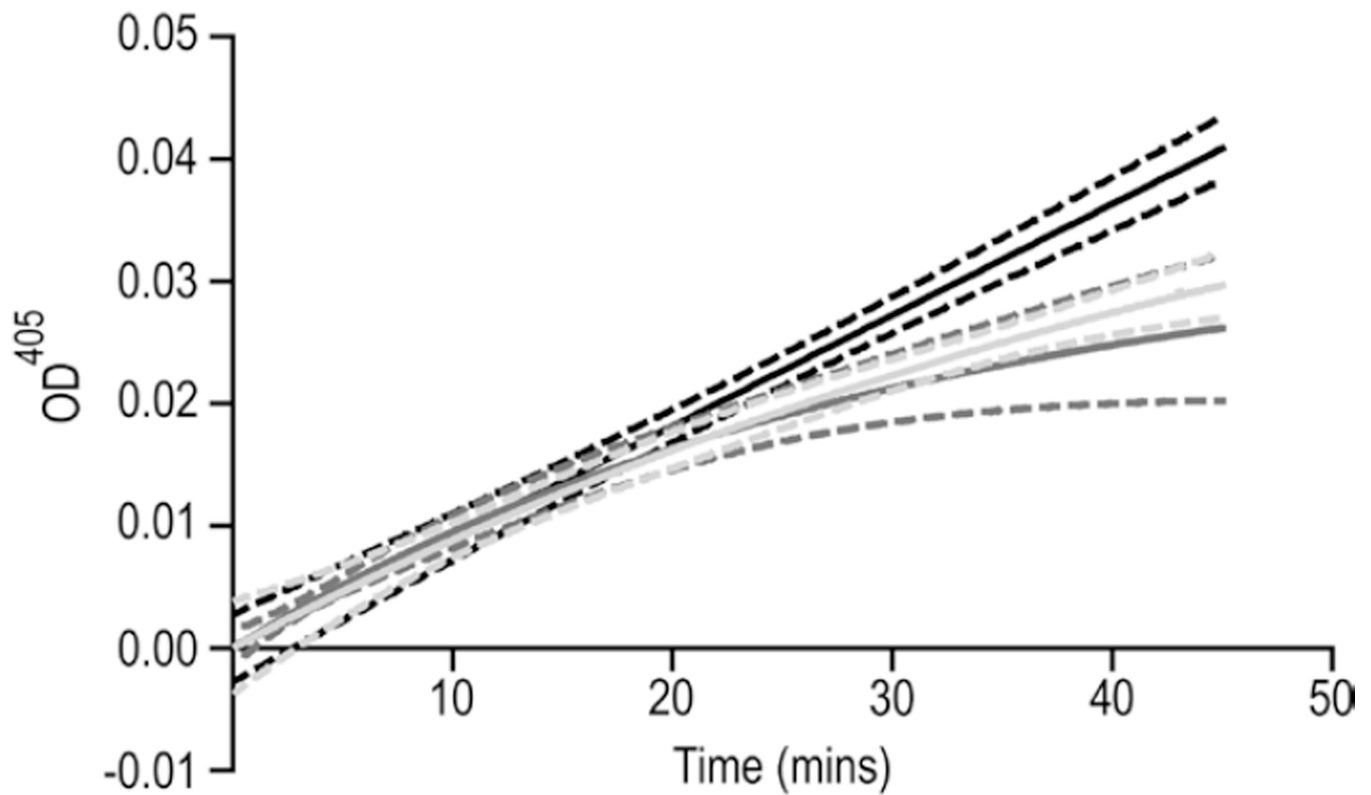


Figure 3. TFPI-GPI and TFPI-TM are equally effective inhibitors of fXa

Factor Xa amidolytic activity was measured in the presence of CHO-TF (black), CHO-TF/TFPI-TM (dark grey), or CHO-TF/TFPI-GPI (light grey) cells, each at 300 $\mu\text{g}/\text{mL}$ total protein. Shown are progress curves fit to a single exponential equation, using GraphPad Prism. Lines represent the mean of six independent experiments. Dashes represent the 95% confidence intervals of the fits.

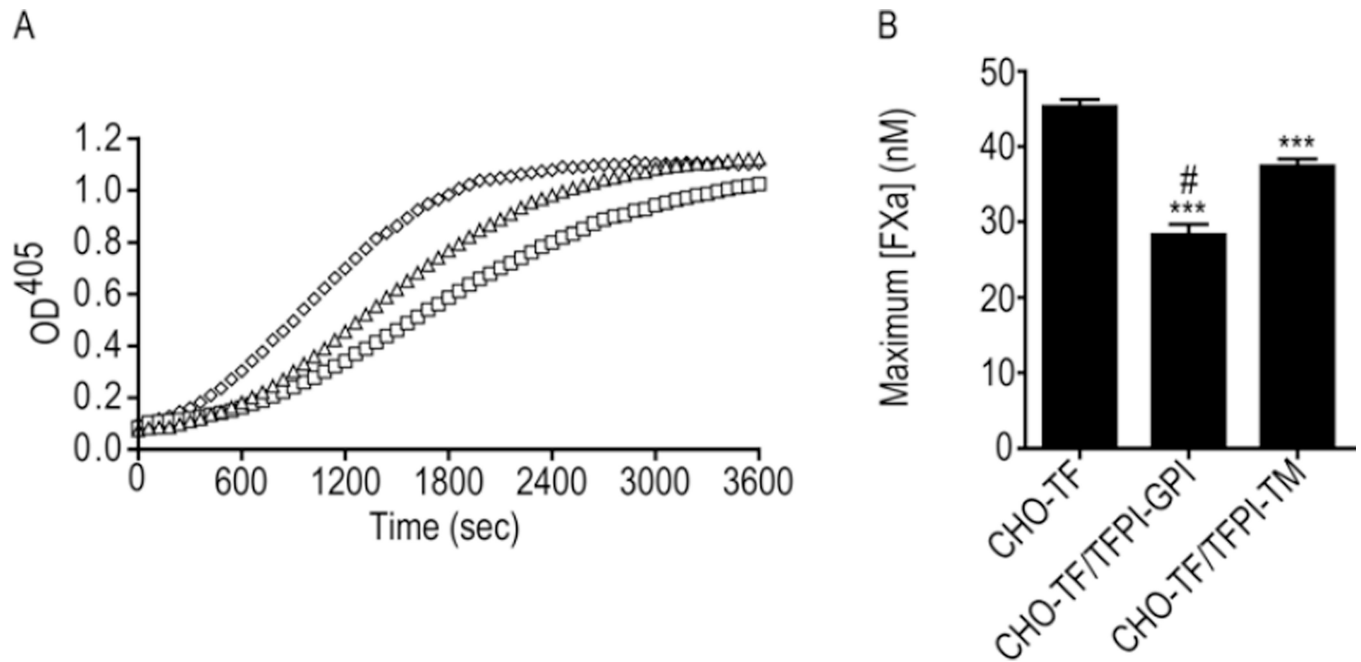


Figure 4. TFPI-GPI is a more effective inhibitor of TF-fVIIa than TFPI-TM

A) Representative progress curves used to determine the maximum amount of fXa generated by TF-fVIIa on the surface of CHO-TF/TFPI-GPI (□), CHO-TF/TFPI-TM (△), or CHO-TF (○) cells, at equivalent concentrations of 300 µg/mL total cellular protein. The plateau observed at an OD of approximately 1.0 represents substrate depletion. B) Maximum amount of fXa (nM) generated by CHO-TF, CHO-TF/TFPI-GPI, or CHO-TF/TFPI-TM cells by TF-fVIIa; mean ± SD, n=4. The assay was performed with cells in suspension. *** - $p < 0.001$ vs. CHO-TF; # - $p < 0.001$ vs. CHO-TF/TFPI-TM.

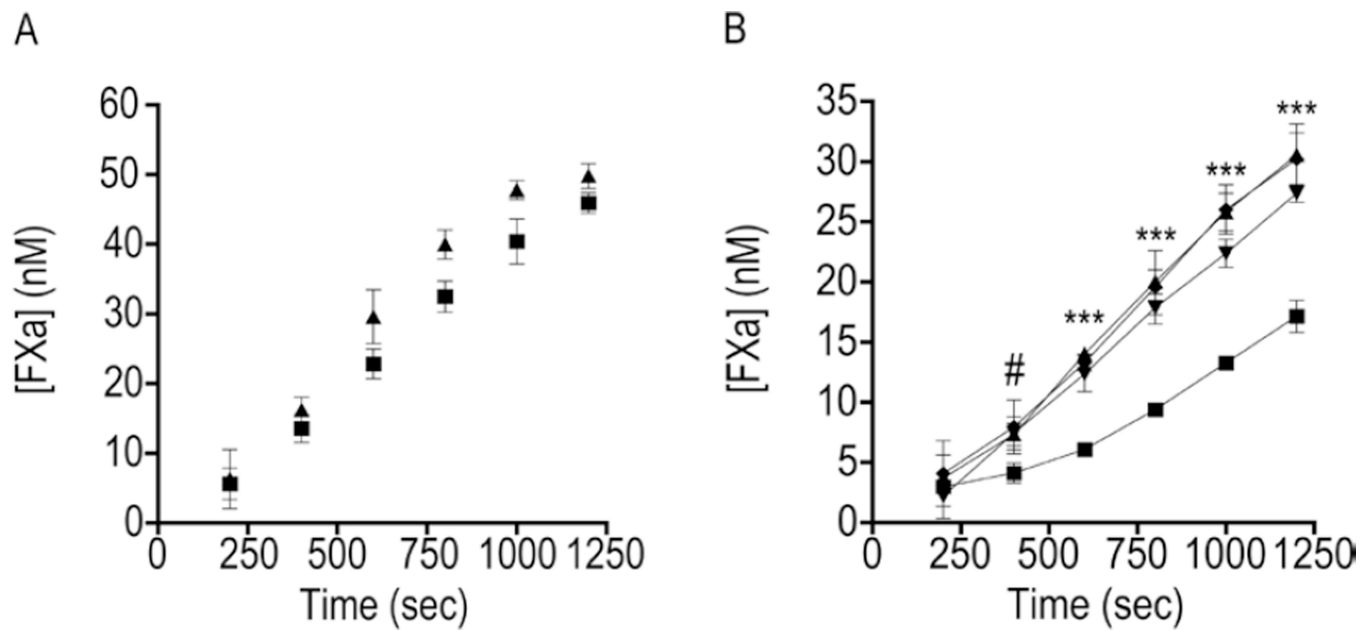


Figure 5. Disruption of caveolae decreases the TF-fVIIa inhibitory activity of TFPI-GPI, but not TFPI-TM

A) Time course of fXa (nM) generation by cholesterol-depleted CHO-TF cells (▲). Treatment with α -cyclodextrin (■) served as a negative control. B) Amount of fXa (nM) generated by cholesterol-depleted CHO-TF/TFPI-GPI and CHO-TF/TFPI-TM cells at different time points. (▼) methyl- β -cyclodextrin and (■) α -cyclodextrin -treated CHO-TF/TFPI-GPI cells; (◆) methyl- β -cyclodextrin and (▲) α -cyclodextrin -treated CHO-TF/TFPI-TM cells. For both figures, the total amount of fXa generated at the end of 200 second intervals of the progress curve are shown (a representative progress curve is presented in Figure 4A). Equivalent cell concentrations of approximately 300 μ g/mL total cellular protein were used for all experiments; mean \pm SD, n=4. The assay was performed with cells in suspension. # - $p < 0.05$ for α -CD- vs. m- β -CD-treated CHO-TF/TFPI-GPI cells. *** - $p < 0.001$ for α -CD- vs m- β -CD-treated CHO-TF/TFPI-GPI cells.

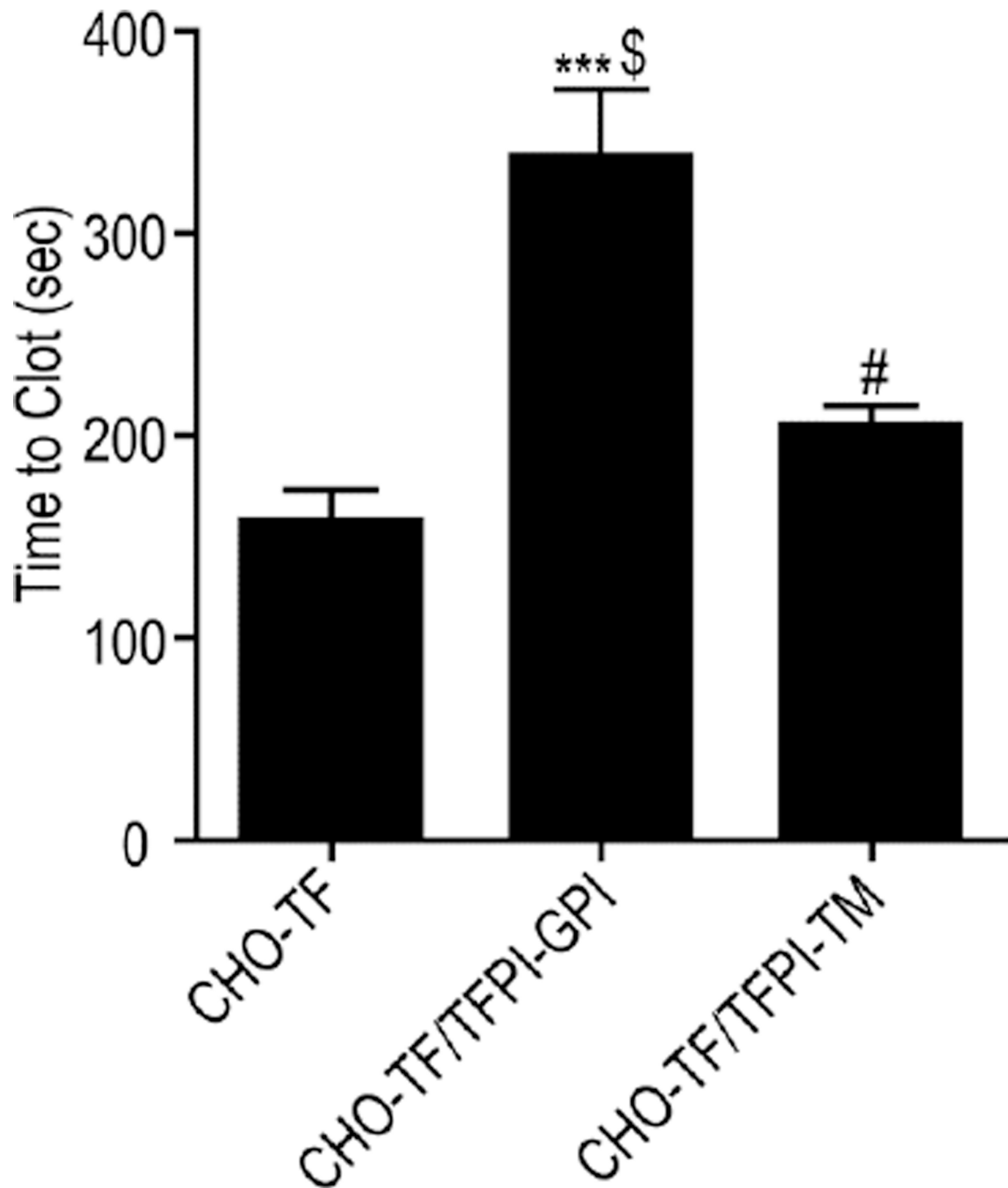


Figure 6. TFPI-GPI is a more effective inhibitor of plasma clot formation than TFPI-TM
Pre-warmed human plasma and CaCl_2 were added to CHO-TF, CHO-TF/TFPI-GPI or CHO-TF/TFPI-TM cells and the time to clot formation recorded; mean \pm SD, $n=4$. The assay was performed with cells in suspension. *** - $p < 0.001$ vs CHO-TF cells; # - $p < 0.05$ vs CHO-TF cells; \$ - $p < 0.001$ vs CHO-TF/TFPI-TM cells.

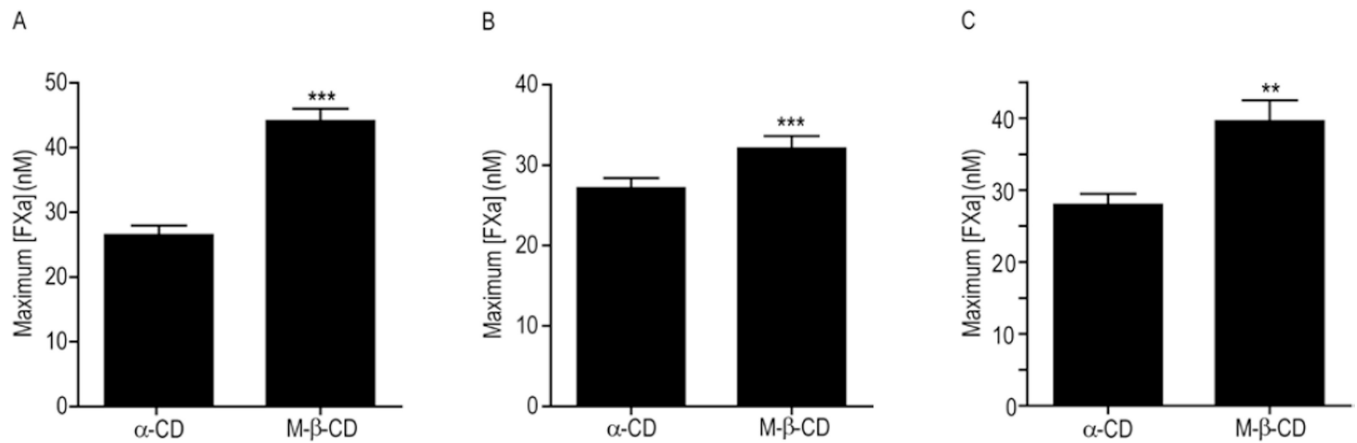


Figure 7. Disruption of caveolae significantly decreases the TF-fVIIa inhibitory activity of endogenous TFPI

Maximum amount of fXa (nM) generated by α -cyclodextrin (α -CD) or methyl- β -cyclodextrin (M- β -CD) treated cells. A) EA.hy926 cells; B) CHO cells transfected with human TFPI β ; C) HUVEC. Equivalent cell concentrations of approximately 300 μ g/mL total cellular protein were used for all experiments; mean \pm SD, n=4 for HUVEC or n=8 for EA.hy926 and CHO-TFPI β . The assay was performed with cells in suspension. ** - $p < 0.01$ vs. α -CD control of the same cell type; *** - $p < 0.001$ vs. α -CD control of the same cell type.

Table 1
Localization of TFPI to caveolae does not affect its fXa inhibitory activity

The fXa inhibitory assay was performed on CHO-TF, CHO-TF/TFPI-TM, and CHO-TF/TFPI-GPI cells in suspension at equivalent concentrations (300 $\mu\text{g}/\text{mL}$ total cellular protein). Numbers represent the mean \pm SD.

Cell Line	Free Factor Xa (nM)	
	Initial	Final
CHO-TF	0.077 \pm 0.041	0.091 \pm 0.035
CHO-TF/TFPI-TM	0.079 \pm 0.019	0.025 \pm 0.020*
CHO-TF/TFPI-GPI	0.083 \pm 0.016	0.019 \pm 0.016 [†]

* - $p < 0.05$ vs. CHO-TF cells;

[†] - $p < 0.01$ vs. CHO-TF cells; $n = 6$.

Table 2
Disruption of caveolae does not affect the fXa inhibitory activity of endogenous TFPI

Cells in suspension were treated with α -cyclodextrin (α -CD) or methyl- β -cyclodextrin (m- β -CD) and the fXa inhibition assay performed at the cellular equivalent of 100 μ g/mL total protein. $p > 0.05$ between α -CD and m- β -CD treated cells of the same cell line, $n = 6$ for each cell line.

Cell Line	Cyclodextrin Tx	Free Factor Xa (nM)	
		Initial	Final
HUVEC	α -CD	0.098 \pm 0.044	0.040 \pm 0.017
	m- β -CD	0.090 \pm 0.025	0.046 \pm 0.012
HB2	α -CD	0.077 \pm 0.016	0.067 \pm 0.031
	m- β -CD	0.090 \pm 0.038	0.061 \pm 0.035
EA.hy926	α -CD	0.082 \pm 0.038	0.060 \pm 0.010
	m- β -CD	0.079 \pm 0.017	0.065 \pm 0.016